A new interpretation of the absorption and the dual fluorescence of Prodan in solution

Cíntia C. Vequi-Suplicy[1,2], Yoelvis Orozco-Gonzalez[1,3], M. Teresa Lamy[1], Sylvio Canuto[1], Kaline Coutinho[1]*

1. *Universidade de Sao Paulo, Instituto de Fisica, 05508-090, Sao Paulo, SP, Brazil.*
2. *Fundacion IMDEA-Nanociencia Cantoblanco, 28049, Madrid, Spain.*
3. *Department of Chemistry, Georgia State University, Atlanta, GA 30302, United States.*

Abstract

Prodan is a fluorescent probe used to monitor biological systems such as lipid membrane, proteins and DNA. Remarkable interest is associated to the interpretation of its fluorescent spectrum. In this paper the sequential hybrid Quantum Mechanics/Molecular Mechanics (S-QM/MM) method was used to establish that the fluorescent emission occurs from two different excited states, resulting in a broad asymmetric emission spectrum with two transitions. The absorption spectra in several solvents were measured and calculated using different theoretical models and they all agree that the first observed band is composed of three electronic excitations very close energetically to each other. The proposed deactivation mechanism in solution indicates that after excitation to the π-π* S_1 excited state, it deactivates via internal conversion to the n-π* S_2 excited state, while S_3 relaxes to its equilibrium geometry. These electronic states were analyzed using multi-configurational calculations (CASSCF) and second-order multi-configurational perturbation theory (CASPT2). It was found that these three excited electronic states are close in energy and the corresponding equilibrium geometries are all planar. In vacuum and in solution the fluorescent states are S_2 (n-π * with a small dipole moment) and S_3 (π-π* with a large dipole moment). A consistent explanation of the experimental data is obtained with the conclusive interpretation that the two transitions observed in the emission spectrum of Prodan, in several solvents, are due to the emission from the S_2 and S_3 excited electronic states.

* To whom correspondence should be addressed:

E-mail: kaline@if.usp.br

Keywords: Prodan, Laurdan, 2-dimethylamino-6-propionylnaphthalene, Photophysics, UV-Vis absorption, dual fluorescence, QM/MM.

I. Introduction

Prodan (2-dimethylamino-6-propionylnaphthalene, Fig. 1) and its derivatives, such as Laurdan, are widely used in biologically relevant systems[1–7] as fluorescent probes. It is very sensitive to the environment with its remarkable emission spectrum shifting by about 120 nm ($6.4x10^3$ cm^{-1} = 0.8 eV) from cyclohexane (λ_{max} = 400 nm = $25.5x10^3$ cm^{-1}) to water (λ_{max} = 520 nm = $19.1x10^3$ cm^{-1}).[1,8–10] Inserted in biological membranes its emission spectra depend on the lipid bilayer phase (gel or fluid), with the wavelength of the maximum of the spectrum shifting by 50 nm (2.4×10^3 cm^{-1}) from one phase to the other.[3,7,11]

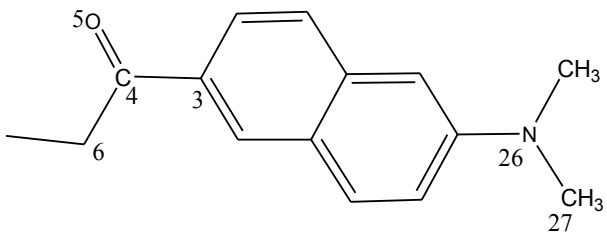

Figure 1: Prodan molecular structure.

The emission spectrum of Prodan is very peculiar because it is broad and asymmetric and is composed by dual emission in several distinct environments, from nonpolar to polar solutions[12–15] and also in biological systems.[7,11,16] The explanation for these dual emission is still a matter of discussion.[17–20] The common hypothesis is that the dual fluorescence comes from only one electronic state, the first excited state S_1, but with a higher emission energy coming from a solvent-non-relaxed S_1 state, so-called locally excited (LE) state, and another with a lower emission energy coming from a solvent-relaxed S_1 state, so-called internal charge transfer (ICT) state. Possibly also with an internal twist of the fluorophore (TICT).[21–37] Other studies recognize some limitations of this hypothesis, suggesting that more investigation is necessary to fully understand the dual fluorescence of Prodan.[8,10,14–19,36,38] Therefore, understanding the origin of the dual emission decay mechanism is critical to improve the applications of Prodan and its derivative as fluorescent probes in biological environments.

It is important to note two consequences of this common hypothesis of the dual emission of Prodan due to the solvent-non-relaxed S_1 state (higher emission energy λ_1^{-1}, locally excited state) and the solvent-relaxed S_1 state (lower emission energy λ_2^{-1}, charge transfer excited state): (i) as the difference between the two emitting states come from the solute-solvent relaxation during the emission process, one should expect a temperature

dependence of the emission spectrum shape due to the different kinetic energy, which induces a faster relaxation and consequently an increase in the fraction of the lower energy emission de-excitation with the increase of temperature (increasing temperature → increasing λ_2^{-1} intensity or area); and (ii) as the relaxed S_1 state is considered to be a charge transfer excited state, one should expect a larger dipole moment that induces a better stabilization in polar solvents and consequently an increase in the fraction of the lower energy emission de-excitation with the increase of solvent polarity (increasing polarity → increasing λ_2^{-1} intensity or area). None of these dependencies were observed experimentally. Indeed, the behavior of the dual emission of Prodan (and its derivative Laurdan) were analyzed with respect to the temperature and the solvent polarity variations in an experimental study.[10] The temperature was changed from 5 to 40°C and no difference was observed in either the emission spectra of Prodan or Laurdan (experimental observation: increasing temperature → no change in λ_1^{-1} and λ_2^{-1}). This experimental information contradicts the first consequence of the common hypothesis discussed above. Additionally, the effect of solvent polarity was analyzed with two different and independent technics used to decompose the emission spectra: the decomposition into two Gaussian bands and the Decay Associated Spectra methodology using time resolved fluorescence. The maxima of the higher energy λ_1^{-1} emission band of Prodan in several solvents were found at 25.5, 23.1, 22.9, 21.4, 20.1 and 19.1 x 10^3 cm^{-1} (393, 433, 437, 467, 496 and 522 nm) for cyclohexane, chloroform, dichloromethane, acetonitrile, methanol and water, respectively. And for the lower energy λ_2^{-1} emission band in the same solvents were found at 24.1, 21.8, 21.5, 20.3, 18.9 and 17.3 x 10^3 cm^{-1} (415, 459, 466, 493, 528 and 579 nm), respectively. Both emission bands are red shifted by increasing the polarity of the solvent from cyclohexane to water, being shifted by $\Delta\lambda_1^{-1}$ = 6.4 x 10^3 cm^{-1} (129 nm) and $\Delta\lambda_2^{-1}$ = 6.8 x 10^3 cm^{-1} (164 nm) (experimental observation: increasing polarity → $\Delta\lambda_1^{-1}$ and $\Delta\lambda_2^{-1}$ red shift). These information can be seen in Fig. 2 where the experimental fluorescent emission spectra of Prodan in cyclohexane and water solutions, obtained in previous work[10], are shown together with the two decomposed band for each solvent. Comparing the maximum intensity of these two decomposed bands, λ_1^{-1} and λ_2^{-1}, and the band areas, it was obtained that the fraction of the lower energy band is higher in cyclohexane than in water, decreasing as the polarity of the solution increases i.e., the intensities are 0.62, 0.54, 0.46, 0.34, 0.24 and 0.15 for the solvents respectively, and the areas fraction are 61%, 52%, 43%, 36%, 26% and 14%, respectively.[10] Therefore, the lower energy λ_2^{-1} emission is destabilized as the solvent polarity increases, i.e. the amount of photons

emitted from the lower energy excited state is smaller in water than in cyclohexane. This finding is in agreement with the previous study performed in ethanol/water mixture[14] and ethanol/buffer mixture.[15] However, it is in conflict with the second consequence of the common hypothesis discussed above. Therefore, a new hypothesis for the dual fluorescence of Prodan (and Laurdan) in homogeneous solvents is possible, where the two emission bands would come from two different excited electronic states.[10,14,15] To verify this possibility, or suggest a new one, Monte Carlo and Molecular Dynamics simulations and quantum mechanics calculations were performed in this work, along with experimental measures of the Prodan spectrum in different solvents. The low-lying excited electronic states and deactivation mechanisms of Prodan were characterized in vacuum and in solvents and also the absorption and emission spectra were computed.

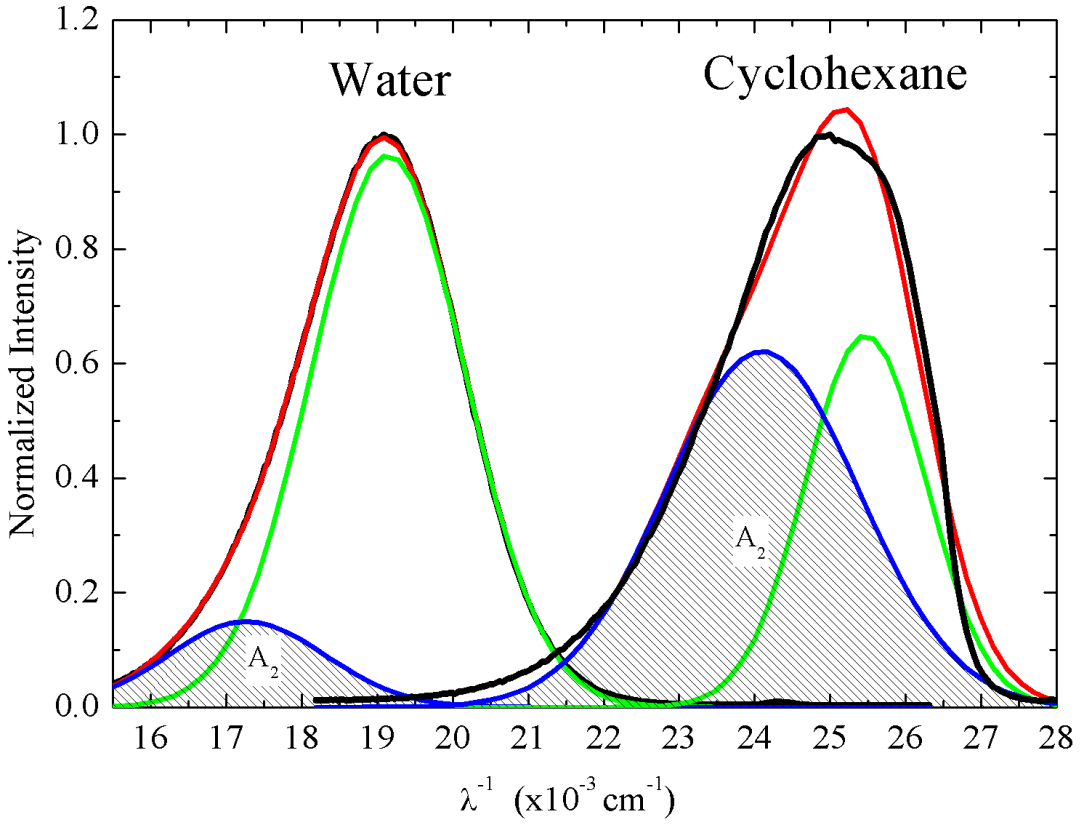

Figure 2: Fluorescent emission spectra of Prodan in cyclohexane and water solutions (in black), Gaussian decomposition: higher energy λ_1^{-1} band (in green), lower energy λ_2^{-1} band (in blue) and total band (in red). Data obtained from ref. 10.

Initially, the electronic transition energies of Prodan in some solvents were calculated and compared with the experimental data of the first band of the UV-visible absorption

spectra. This motivated us to obtain again the experimental absorption spectrum and analyze also the broadening of the band. An excellent agreement was found between the theoretical results and the experimental data and the important conclusion obtained from this comparison was the existence of three electronic excitations in the first absorption band. Therefore, by exciting Prodan at the wavelength of the maximum absorption of the first band, our calculations show that it is possible to populate three different excited states. These combined theoretical and experimental results along with the characterization of the low-lying excited electronic states of the Prodan will be used to support the hypothesis that Prodan fluorescent emission is due to the decay of two independent states that are accessible in the absorption band and can be populated when Prodan is excited with energies around 27.8-29.5 x 10^3 cm^{-1} (360-340 nm). These two states are characterized with quantum mechanics (QM) calculations using different theoretical levels ranging from semi-empirical to multi-configurational perturbation theory.

II. Experiment

To assist and complement our theoretical results for the absorption spectra of Prodan in different solvents these spectra were measured experimentally in this work.

Materials and methods

The fluorophores Prodan and Laurdan were purchased from Molecular Probes Inc. (Eugene, OR, USA) and the solvents cyclohexane, chloroform, dichloromethane, acetonitrile and methanol from Sigma-Aldrich (St Louis, MO, USA). Water was Milli-Q Plus (Millipore), pH ~ 6.0. Stock solutions of the fluorophore in chloroform (1.5 mM) were used in all experiments. Appropriated amounts of these solutions were transferred to glass flasks using calibrated glass microsyringes. Chloroform was evaporated under a stream of dry N_2. The dry residue was dissolved in the desired solvent to obtain the fluorophore concentration of 4.0 μM. pH was measured for all samples in water, and no change was observed (pH ~ 6.0).

The electronic absorption spectra were measured with a Cary-50 spectrophotometer (Varian Australia PTY LTD, Mulgrave, VIC, Australia) with temperature fixed at 25 ± 1^oC with a Single Cell Peltier temperature controller. All data shown are averages of at least three experiments.

III. Computational Details

Absorption and emission spectra

The absorption spectra were calculated using four different methods: (1) Time Dependent Density Functional Theory (TD-DFT)[39] using the B3LYP functional and 6-311G(d) basis set with the solvent treated as polarizable continuum model (PCM).[40] This method will be called TD-B3LYP/PCM; (2) Semi-empirical Intermediate Neglect of Differential Overlap with single excitations in the Configuration Interaction method (INDO-CIS) using the original spectroscopic parameterization[41] with the solvent included as Self-Consistent Reaction Field (SCRF)[42,43]. This method will be called INDO-CIS/SCRF; (3) Semi-empirical INDO-CIS with the solvent included as explicit molecules using solute-solvent configurations obtained from Molecular Mechanics simulation with either methods: Molecular Dynamics (MD) or Monte Carlo (MC). This method will be called INDO-CIS/Explicit. It uses several solute-solvent configurations characterizing the solution at a specific thermodynamic condition. Then, naturally it provides inhomogeneous contribution to the band broadening. The details of the simulations are given below; (4) Single-state second order multi-configurational perturbation theory (CASPT2)[44] based on a multi-state Complete Active Space Self-Consisted Field (CASSCF) wave function.[45] This method was used to compute the absorption spectrum of the Prodan, but also to characterize the low-lying excited electronic states and compute the emission spectrum, both in vacuum and in water solution treated with ASEC. This method will be called CASPT2/ASEC. The active space of CASSCF calculations correlates 12 electrons in 12 orbitals, termed as CASSCF(12,12). The active orbitals are the five π and six π^* that better describe the two lowest π-π^* excited states and it was added the oxygen lone-pair orbital to describe the lowest n-π^* excited state. The ANO-L basis set[46,47] was used with the contraction scheme C, O and N (14s9p4d)/[4s3p1d], H (8s4p)/[2s1p]. The ground and excited electronic states were optimized at the same level, using CASSCF/ANO-L-4s3p1d/2s1p in vacuum.

The ground state equilibrium geometry of the Prodan was previously obtained by Vequi-Suplicy *et al.*[48] This planar geometry, generated with DFT/B3LYP/6-31G(d) level, does not show significant changes when optimized in vacuum or in solution (treated as PCM). This behavior persisted even using two additional basis sets (6-311+G(d) and aug-cc-pVDZ). For comparison with previous result this geometry were also used in the calculation

of the absorption spectrum of Prodan in solution with three methods: TD-B3LYP/PCM, INDO-CIS/SCRF and INDO-CIS/Explicit.

All the semi-empirical calculations were performed with the ZINDO program,[49] the DFT calculations were performed with the Gaussian03 program package[50] and the multi-configurational calculations were performed with the MOLCAS 7.6 program package.[51]

Molecular mechanics simulations

The solvent effects in the electronic states (ground and excited states) and in the transition energies were taken into account using the sequential Quantum Mechanics/Molecular Mechanics (S-QM/MM) methodology,[52–54] unless PCM were stated. The Molecular Mechanics simulations were performed using the standard Monte Carlo (MC) method with the Metropolis sampling technique[55] with the solute rigid in the optimized geometry. Nevertheless, to take into account the effect of the intramolecular degree of freedom, Molecular Dynamics (MD) was also performed. The MD flexibility is expected to mostly affects the C=O stretch in water due to the formation of hydrogen bonds and possible rotations between the aromatic ring and the other groups. The isothermal-isobaric *NPT* ensemble at room temperature and pressure conditions (298 K and 1 atm) was used in both the MC and MD simulations. One Prodan and 1000 water molecules or 500 molecules of the other solvents (acetonitrile, dichloromethane and cyclohexane) were considered in a rectangular box with periodic boundary conditions and minimum image method. The intramolecular parameters of Prodan used in flexible simulation were obtained from the all-atom Optimized Potentials for Liquid Simulations (OPLS/AA) force field.[56] However, the equilibrium bond distances and angles were used from the optimized geometry with QM calculation with B3LYP/6-31G(d) level and the rotational angles between the aromatic rings and the -$N(CH_3)_2$ and the -$COCH_2CH_3$ groups ($\varphi_{O-C-C-C}$, $\varphi_{C-N-C-C}$ and $\varphi_{H-C-N-C}$) were reparametrized to describe QM energy profile with the same level. The intermolecular interactions were described by the Lennard-Jones plus Coulomb potentials with three parameters for each interacting site (ε_i, σ_i and q_i for an atom i). The Lennard-Jones, ε_i and σ_i, parameters for the Prodan were obtained from the all-atom Optimized Potentials for Liquid Simulations (OPLS/AA) force field[56] and the atomic charges, q_i, of the Coulomb potential were obtained with QM calculations polarized in the presence of the solvent with an iterative-QM/MM polarization procedure.[57–59] The iterations allow obtaining new solute atomic charges that converges to the polarized electrostatic equilibrium with the solvent distribution. The implementation uses the Average Solvent Electrostatic Configuration (ASEC)[60] to

describe the solvent distribution and the atomic charges for the solute for each iterative-QM/MM step is obtained with the CHELPG procedure[61] for the electrostatic fitting calculated at MP2/aug-cc-pVDZ level for the ground state and with the ElectroStatic Potential Fitted method (ESPF)[62] at the CASSCF/ANO-L level for the ground and excited states. Then, for both QM levels (MP2 and CASSCF), an ASEC electrostatic embedding of the solvent was used to include the electronic polarization of the solute in different solvents. And also, an iterative procedure was performed for each excited electronic state (only with CASSCF) to obtain the Prodan electron density in electrostatic equilibrium with the water solution.[57,63]

The geometry and the parameters used for the solvents were: the simple point charge model (SPC/E)[64] for water; the Bohm *et al* [65] parameters for acetonitrile; and the OPLS-AA[56] for dichloromethane and cyclohexane in the chair conformation.

The MC simulation consisted of a thermalization stage of 1.2×10^8 MC steps, followed by an equilibrium stage of 1.5×10^8 MC steps, where in each step one molecule was randomly selected to translate and rotate according to the Metropolis sampling technique. A thermalized configuration obtained from the MC simulation was used to start the MD simulations. A thermalization phase of 3 ns was performed to equilibrate the kinetic and potential energy and the MD simulation was carried out for more 6 ns. The time step was 0.1 fs. To solve the equations of motion the integrator method was the velocity-Verlet.[66] To keep the temperature and pressure constant, Berendsen thermostat and barostat were used.[67] All the MC simulations were performed with the DICE program[68,69] and the MD was performed using the TINKER program.[70,71]

After the simulations a statistical analysis was performed[53] and 100 statistically uncorrelated configurations (less than 10% of statistical correlation) of the system were selected and submitted to QM calculations of the absorption energies. The configurations selected for the QM calculation were composed by one Prodan molecule, the first solvation shell as explicit solvent molecules and the second solvation shell treated as an electrostatic embedding using the atomic charges of the solvent molecules (obtained from the classical force field). The calculations were first performed using the semi-empirical INDO-CIS method considering all occupied and unoccupied valence orbitals, i.e., a full CIS considering 43 occupied orbitals and 44 unoccupied. Another set of QM calculations was performed with 100 statistically uncorrelated configurations to generate ASEC where all solvent molecules are treated as an electrostatic embedding described by atomic point charges.[60,63,72] When using ASEC, a single configuration represents the average of all solvent configurations and it

takes into account the electrostatic embedding of the solvent environment. This make possible to compute properties of the excited electronic states in a very efficient way considering the effect of the environment.

IV. Results and Discussions

Geometry, polarization and solvation

The optimized geometry of Prodan in the ground state obtained with the B3LYP/6-31G(d) method is a planar structure with a small bending of the methyl groups bonded to the nitrogen atom ($\varphi_{C-N-CH_3-CH_3}$= 165.3°) in good agreement with the X-ray crystallographic structure.[30] The calculated value of the dipole moment is 5.8 D in vacuum with MP2/aug-cc-pVDZ (see Table 1). In the solvent environment it naturally increases to 6.1 D, 7.7 D, 8.0 D and 10.2 D in cyclohexane, dichloromethane, acetonitrile and water, respectively, as discussed before.[48] The polarization of Prodan due to the presence of the solvent environment increases with the solvent polarity and the effect of the water is remarkable with an increase of 76%. Analyzing the charge distribution of the Prodan in vacuum (non-polarization), there is a small charge separation between the electron donor and acceptor groups (q_i(N)–q_i(O) = 0.16 *e*) but a large local charge separation in the C=O bond (q_i(C)–q_i(O) = 0.80 *e*). In solution, the charge separation between the electron donor and acceptor groups increases with the solvent polarity (q_i(N)–q_i(O) = 0.25, 0.30, 0.26 and 0.47*e*, for cyclohexane, dichloromethane, acetonitrile and water, respectively), and the local charge separation in the C=O bond increases even more (q_i(C)–q_i(O) = 0.99, 1.10, 1.06 and 1.36 *e*, respectively). The electronic distribution of Prodan is very sensitive to the environment and hence subjected to considerable polarization.

The geometry of the ground state obtained with CASSCF/ANO-L is similar to the one optimized with the B3LYP/6-31G(d) method discussed above. The vertical excited states (in the S_0 equilibrium geometry) S_1, S_2 and S_3 are close in energy, within 0.3 eV (2.2 x 10^3 cm^{-1}), but they have quite different electronic structure that leads to the dipole moments of 5.7, 1.5 and 11.4D, respectively. Therefore, comparing their dipole moment with the ground state state S_0 (5.3D), the S_1 state has a similar value, the S_2 has a much smaller value and the S_3 has a much larger value. These three excited states relax to their equilibrium geometry stabilizing by 0.3, 1.2 and 0.7 eV, respectively. The geometry differences of the relaxed low-lying excited states compared to the ground state are small, mostly the planarity of the amino

group and the C=O distance. The S_1, S_2 and S_3 equilibrium geometries are fully planar, i.e., with planar improper dihedral angle between the methyl groups bonded to the nitrogen atom and the aromatic rings, $\varphi_{C-N-CH_3-CH_3}$= 179° for S_1 and 180° for S_2 and S_3. Moreover, the C=O distances are d_{CO}= 1.225 Å for S_0, 1.210 Å for S_1, 1.357 Å for S_2 and 1.216 Å for S_3. Additionally for the S_2 geometry, there are variations of the related angles, such as θ_{O-C-CH_2}= 120° for S_0, S_1 and S_3 and 113° for S_2. The main difference between the equilibrium geometry of the S_3 and S_1 is a small reduction in the distance of the nitrogen atom and the carbon of the rings, d_{NC}= 1.385 Å for S_1 and 1.339 Å for S_3. The Cartesian coordinates of these four equilibrium geometries (S_0, S_1, S_2 and S_3) are presented in the Supporting Information (SI). The geometry optimizations and the minimum energy path (MEP) for the three low-lying excited states were performed also in geometries with rotations at the -$N(CH_3)_2$ and -$COCH_2CH_3$ groups. But the planar geometries were found to be the most stables, with lower energies.

Table 1. The atomic charges (in *e*) of some atoms, C=O and N, and the dipole moment (in D) of Prodan in vacuum and in aqueous solution are shown. The values are calculated for the ground state (S_0) and for the three low-lying relaxed excited states (S_1, S_2 and S_3) with CASSCF/ANO-L/ESPF. In parentheses are shown the values for the vertical excited states. For comparison the atomic charges of the S_0 were also calculated with MP2/aug-cc-pVDZ/CHELPG. For all calculation in water the polarization were obtained using the ASEC electrostatic embedding.

	S_0 (MP2)	S_0 (CASSCF)	S_1 (CASSCF)	S_2 (CASSCF)	S_3 (CASSCF)
Vacuum					
q_i(C)	0.36	0.34	0.48	0.04	0.37
q_i(O)	-0.44	-0.42	-0.59	-0.15	-0.52
q_i(N)	-0.28	-0.18	-0.07	-0.03	-0.03
μ	5.8	5.3	5.8 (5.7)	1.6 (1.5)	11.2 (11.4)
In water					
q_i(C)	0.60	0.86	0.66	-0.10	0.45
q_i(O)	-0.76	-0.88	-0.87	-0.22	-0.89
q_i(N)	-0.29	-0.09	-0.05	-0.21	-0.17
μ	10.2	9.1	9.7 (9.7)	2.9 (4.8)	17.2 (17.9)

Using the equilibrium geometry for each one of the four electronic states of Prodan, the charge distribution was calculated in vacuum and in aqueous solution with CASSCF/ANO-L/ESPF. The calculated values of the dipole moment were 5.3, 5.8, 1.6 and 11.2 D in vacuum for S_0, S_1, S_2 and S_3, respectively (see Table 1). Therefore, the geometry

relaxation has only a small effect in the dipole moment of the excited states compared with the vertically excited states (in the S_0 geometry). In the other hand, the solvent effect is considerable. Their dipole moments in water are 9.1, 9.7, 2.9 and 17.2 D in water for S_0, S_1, S_2 and S_3, respectively. These values are also presented in Table 1 together with some relevant atomic charges. The complete sets of atomic charges are presented in the SI. Comparing the ground state S_0 with the S_1, S_2 and S_3 excited states, it was found that the S_1 state has a dipole moment slightly larger than the S_0 (5.8 and 5.3 D in vacuum and 10.2 and 9.1 D in water), but the S_2 state has a large decrease, μ = 1.6 D in vacuum and 2.9 D in water, and the S_3 state has a large increase, μ = 11.2 D in vacuum and 17.2 D in water.

The solvation shells around Prodan is determined using the minimum distance distribution function (MDDF)[72,73] and the effect of the polarization of the solute due to the solvent is analyzed. The MDDFs between Prodan in the ground state S_0 and the four solvents studied are presented in the SI. Also shown in the SI are the MDDF for the three excited states in water. For the solvents cyclohexane, dichloromethane and acetonitrile, no significant changes were observed in the average solvation shells using the non-polarized and polarized sets of atomic charges of Prodan using MP2/aug-cc-pVDZ/CHELPG. However, for the aqueous solution, although the number of water molecules in the solvation shells remains the same, an increase in the number of hydrogen bonds was observed. The quantity of solvent molecules in the first and second solvation shells was 20 (up to 4.15 Å) and 77 (from 4.15 to 9.35 Å) for cyclohexane, 24 (up to 4.65 Å) and 80 (from 4.65 to 8.55 Å) for dichloromethane, 29 (up to 4.15 Å) and 100 (from 4.15 to 7.95 Å) for acetonitrile and 56 (up to 4.05 Å) and 231 (from 4.05 to 7.95 Å) for water. For the polarized Prodan in water, it is possible to observe a small peak in the MDDF around 1.70 Å that is characteristic of hydrogen bonds (HBs) between Prodan and water molecules. The number of water molecules in the solvation shells is still the same for the four electronic states, S_0, S_1, S_2 and S_3, but the number of HBs differs.

Absorption spectra

The experimental absorption spectra of the fluorophore Prodan and Laurdan in six solvents are presented in SI. In Fig. 3 only the first absorption band is shown along with the calculated excitation energies. As it can be seen this band is very broad in all solvents. Therefore, when referring to the experimental value one should consider that this is the band maximum of a considerably broad absorption band.

The results obtained with INDO-CIS/SCRF and TD-B3LYP/PCM for the first three excitations are presented as vertical lines in Fig. 3. For the INDO-CIS/Explicit the excitations were calculated for 100 solute-solvent configurations obtained from the simulations. This leads naturally to band broadening and the three calculated excitations are presented in Fig. 3 as histograms, giving a very good description of the observed band. In the case of water the solute-solvent configurations were generated with two simulation methods, MC and MD. The difference between them is the flexibility of the solute. As it can be seen in Fig. 3, the outcome of 100 QM calculations with the INDO-CIS/Explicit using solute-solvent configurations obtained from MC simulation (with rigid solute) present a broadening caused by the diversity of solvent positions around the solute and in the case of MD simulation (with flexibly solute) presents an even broader distribution of excitation energy due to the solute deformation. This describes very well the broadening of this first absorption band in water. Analyzing the Prodan conformations during the MD simulation, the planarity was maintained with rotational angles variations between the aromatic rings and the $-N(CH_3)_2$ and the $-COCH_2CH_3$ groups around $\pm 15^o$, but mostly the deformation comes from the C=O stretch caused by the hydrogen bond formed between the Prodan and the water molecules. In cyclohexane, dichloromethane and acetonitrile we see the separation of the first three excitations (solid histogram in blue for the n-π^* and in red for the π-π^*) of 100 solute-solvent configurations obtained with MC simulation.

All methods used in this work agree that the first experimental band is composed of three excitations: one n-π^* and the two π-π^* transitions. In nonpolar environments (vacuum, cyclohexane and dichloromethane), the INDO-CIS/Explicit, INDO-CIS/SCRF and the TD-B3LYP/PCM calculations show the n-π^* as the first transition followed by the two π-π^*. In polar solvents (acetonitrile and water), the n-π^* transition becomes the second excited state. This is easy to understand because in more polar solvents the n-π^* transition shifts to the blue (higher energy) whereas the π-π^* transitions shift to the red (lower energy). This is summarized in Table 2. The experimental excitation energies (and wavelengths) presented at Table 2 correspond to the maximum absorption. However, to compare with the theoretical results it is important to consider the large broadening of this band as seen in Fig. 3.

Table 2: Calculated vertical excitation energies for Prodan in vacuum and in different solvents calculated with four different methods. In the case of explicit solvent the values were obtained with average over 100 solute-solvent configurations selected from MC simulations for all solvents except for water that is from MD simulation. The values are in 10^3 cm^{-1} and in parentheses in nm. The experimental values are the band maximum shown in Fig. 3 and obtained in this work. The asterisk indicates n-π* transition.

Excitation	Vacuum	Cyclohexane	Dichloromethane	Acetonitrile	Water
Method: INDO-CIS/Explicit					
1st	-	26.6±0.1 (376)*	26.9±0.3 (372)*	26.2±0.3 (382)	27.2±1.2 (368)
2nd	-	29.0±0.1 (345)	28.5±0.5 (351)	28.5±0.5 (351)*	28.5±0.7 (351)*
3rd	-	30.2±0.1 (331)	30.0±0.3 (333)	30.7±0.3 (326)	28.5±1.1 (351)
Method: INDO-CIS/SCRF					
1st	26.7 (375)*	26.9 (372)*	27.6 (362)*	27.6 (363)	27.5 (364)
2nd	29.1 (343)	28.8 (347)	28.0 (357)	27.9 (359)*	27.9 (358)*
3rd	30.0 (333)	30.0 (333)	29.1 (343)	29.1 (344)	28.8 (348)
Method: TD-B3LYP/PCM					
1st	28.0 (370)*	27.1 (370)*	26.5 (377)*	26.4 (379)	26.4 (379)
2nd	30.3 (331)	29.9 (334)	29.5 (339)	29.4 (340)*	29.4 (340)*
3rd	30.3 (330)	30.8 (325)	31.5 (318)	32.0 (313)	31.7 (316)
Method: CASPT2/ASEC					
1st	31.9 (313)	-	-	-	30.6 (327)
2nd	32.0 (313)*	-	-	-	31.9 (313)
3rd	34.4 (291)	-	-	-	33.5 (299)*
Exp.	-	29.1 (344)	28.2 (354)	28.2 (354)	27.6 (362)

The excitation energies (Table 2) calculated with CASPT2/ASEC are larger than those calculated with B3LYP/PCM or the two INDO-CIS models used and also the experimental data. Comparing CASPT2 with B3LYP, the n-π* excitation in water differs by 4.1 x10^3 cm^{-1} (40 nm) and becomes the third excitation after a blue shift of the second excitation in vacuum. In changing from vacuum to water the n-π* excitation is blue shifted by 1.5 x10^3 cm^{-1}. This value is comparable to the blue shifts obtained with the other theoretical models, shown in Table 2. In spite of obtaining large excitation energies the results at the CASPT2 level agree that the first observed band should be composed of three low-lying transitions. The separation between these three transitions amount to 3.0 x10^3 cm^{-1} and is still much less that the broadening experimentally observed to the first absorption band. Then, we conclude that all theoretical models adopted here agree that the first absorption band of Prodan in solution is composed by vertical excitations from the ground state to three different excited states, one n-π* and two π-π* states.

There are several previous studies that report theoretical results of the absorption energies of Prodan in vacuum.[20,22,30,31,74] Most of these results underestimate the first transition and overestimate the second when compared with the results in Table 2. Two previous papers,[19,36] using the PCM model for the solvent obtained results that are in good agreement with the experimental data. Therefore, considering Fig. 3 and Table 2, it is

possible to conclude that the absorption spectra of Prodan in all the solvents considered are well described by three electronic excitations.

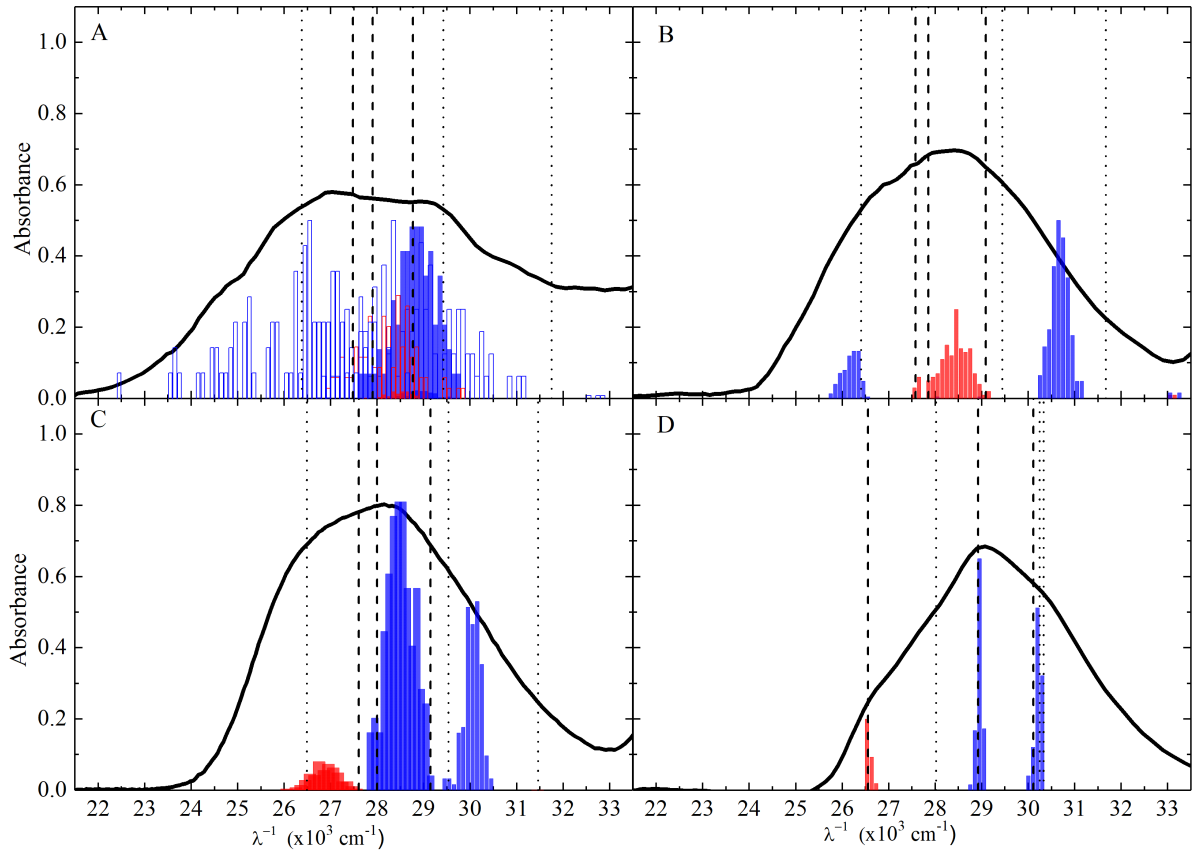

Figure 3: Absorption spectra of Prodan in several solvents: (A) in water, (B) in acetonitrile, (C) in dichloromethane and (D) in cyclohexane. Black solid line is the experimental result (this work). Vertical lines are the first three excitations calculated with INDO-CIS/SCRF (dashed) and with B3LYP/PCM (dotted). The histograms (in red is n-π^* and in blue is π-π^* excitations) are the excitations calculated with INDO-CIS/Explicit for 100 different solute-solvent configurations obtained with MC simulations for all solvent (solid histogram) and with MD simulation (open histogram) only for water.

The excited electronic states and the emission spectrum

To analyze the excited states of Prodan we use the more adequate CASSCF and CASPT2 methods. The low-lying excited electronic states were first identified from the absorption transitions computed at the CASPT2 level in vacuum. Three relevant excited electronic states were identified. The S_1 state is a π-π^* electronic state mainly described by the transitions HOMO-1→LUMO and HOMO→LUMO+1, while S_2 is a n-π^* excited electronic state characterized by the transition from the oxygen lone-pair orbital to the LUMO+1 and S_3 also shows a π-π^* character mainly described by the HOMO→LUMO transition. The molecular orbitals characterizing these electronic states are shown in Fig. 4.

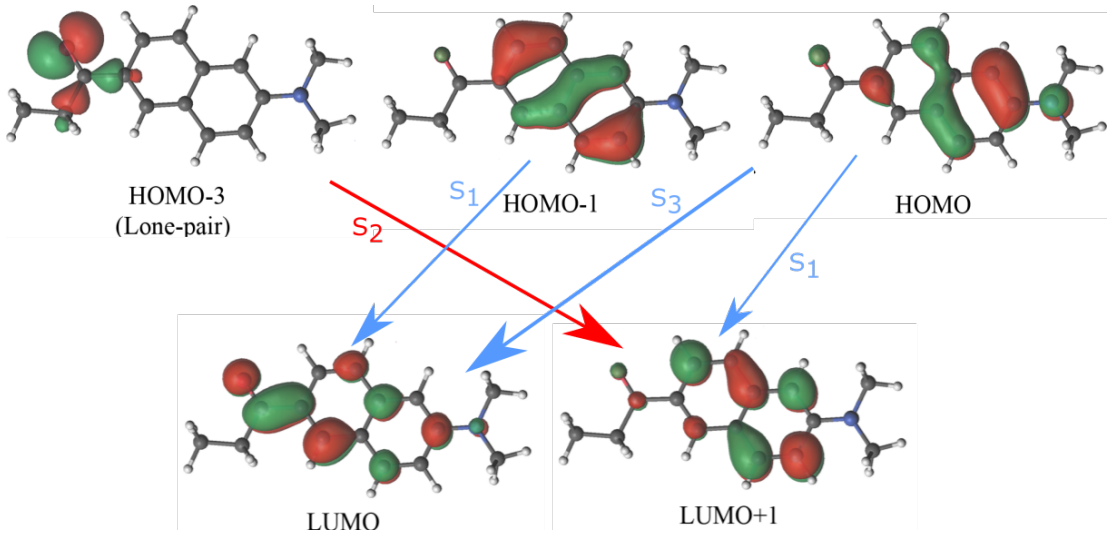

Figure 4. Molecular orbitals involved in the electron transition of the three lowest excited electronic states.

To better analyze the photophysics of Prodan in vacuum and in water solution, the absolute energy of the three excited electronic states were recalculated with CASPT2 level using the equilibrium geometries obtained with CASSCF(12,12) level. This method will be called CASPT2//CASSCF. With these results the minimum energy paths (MEP) are built and they are schematically represented in Fig. 5. The transition energies are presented in Table 3. In Fig. 5A, the photophysics of Prodan in vacuum is schematically summarized. The grey region indicated in Fig. 5A seems to be a very important characteristic of this molecular system, since excitation energies from about 31.9 to 34.2 x10^3 cm^{-1} (292 to 313 nm) could populate these three excited electronic states, as they are very close energetically to each other. Taking into account that the S_2 excited state is a dark state due to the weak oscillator strength of the n-π^* electronic transition, it is expected that S_1 and S_3 are the main populated states upon the Franck-Condon absorption transition. Following the MEP of the S_1 state, it can be observed that the S_2 state is very close energetically, just 100 cm^{-1} (2 nm) above. This condition is very favorable for an internal conversion decay from S_1 to S_2, which at its corresponding equilibrium geometry is the most stable of the three excited states. On the other hand, the MEP of the S_3 state presents another equilibrium geometry. As a result, it is expected to observe two fluorescent transitions for the Prodan molecular system, corresponding to the emission of the excited electronic states S_3 at higher energy λ_1^{-1} = 28.9 x10^3 cm^{-1} and S_2 at lower energy λ_2^{-1} = 22.5 x10^3 cm^{-1}.

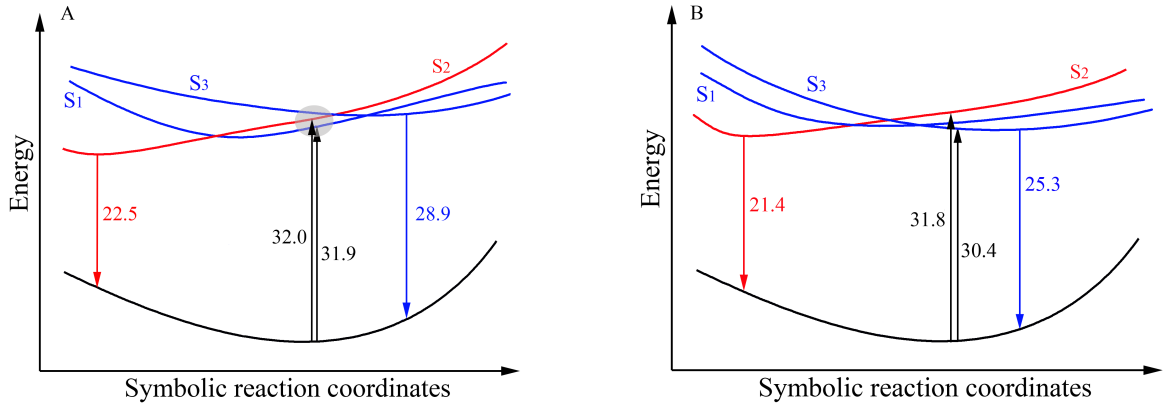

Figure 5. Schematic representation of the photophysics of the Prodan in vacuum (A) and in water (B) with transition energies presented in 10^3 cm^{-1}.

Table 3. Transition energies of Prodan calculated at the CASPT2//CASSCF level in vacuum and in water using PCM and the electrostatic embedding ASEC model obtained with MC simulations. In bold, the emissions of the states S_1, S_2 to S_3 to the ground state S_0 were highlighted. Values are in 10^3 cm^{-1} and in parentheses in nm.

	Vacuum	PCM (water)	ASEC (water)
Franck Condon S_0 geometry			
$S_1 - S_0$	31.9 (314)	31.9 (313)	31.3 (320)
$S_2 - S_0$	32.0 (312)	33.6 (298)	31.8 (315)
$S_3 - S_0$	34.2 (292)	30.6 (327)	30.4 (328)
S_1 equilibrium geometry			
$S_1 - S_0$	**29.7 (336)**	**29.3 (342)**	**29.3 (341)**
$S_2 - S_0$	29.9 (334)	31.5 (317)	32.4 (308)
$S_3 - S_0$	33.5 (299)	30.8 (325)	30.1 (332)
S_2 equilibrium geometry			
$S_1 - S_0$	30.4 (329)	30.4 (329)	31.1 (329)
$S_2 - S_0$	**22.5 (444)**	**24.8 (403)**	**21.4 (467)**
$S_3 - S_0$	31.5 (317)	27.5 (364)	36.1 (277)
S_3 equilibrium geometry			
$S_1 - S_0$	29.2 (343)	30.3 (330)	26.0 (384)
$S_2 - S_0$	31.7 (315)	31.7 (316)	33.0 (303)
$S_3 - S_0$	**28.9 (346)**	**27.3 (367)**	**25.3 (395)**

Characteristic shifts of the transition energies are observed when the solvent effect is taken into account, using the solvent represented as a continuum dielectric (PCM) or discrete electrostatic embedding (ASEC), as shown in Table 3 and Fig. 5B. In the presence of the solvent the photophysical behavior previously described is still valid. The main difference, as shown in Table 3, is the solvatochromic shift of the S_3 emission, showing the largest red shift of 3.6 x 10^3 cm^{-1} (49 nm) from 28.9 x 10^3 cm^{-1} in vacuum to 25.3 x 10^3 cm^{-1} in water. This is explained by the large dipole moment of S_3 in comparison with the ground state S_0 (see Table 1). Moreover, the solvatochromic shift of the S_2 emission is also red shifted by 1.1 x 10^3 cm^{-1}

(23 nm) from 22.5 x 10^3 cm^{-1} in vacuum to 21.4 x 10^3 cm^{-1} in water. This red shift is a characteristic behavior because the dipole of the S_2 state is smaller than in the S_0 state and this should generate a larger stabilization of the S_0 state in water causing a blue shift comparing with the calculation in vacuum. However these red shifts of the two fluorescent states are in qualitative agreement with the experimental data.[10,14,15] The experimental shift[10] changing from cyclohexane to water was shown in Fig. 1, $\Delta\lambda_1^{-1}$ = 6.4 x 10^3 cm^{-1} (129 nm) for the higher energy emission and $\Delta\lambda_2^{-1}$ = 6.8 x 10^3 cm^{-1} (164 nm) for the lower energy emission. For the S_1 electronic transition, small or no shifts are observed because the dipole moments of the S_0 and S_1 electronic states are similar.

Although the computed emission energies in water (λ_1 = 395 nm for S_3 and λ_2 = 467 nm for S_2) are not in quantitative agreement with the experimental results[10] (λ_1 = 522 nm and λ_2 = 579 nm) showing differences of 127 and 112 nm, respectively, the calculated separation between the two emission λ_1 and λ_2 of 72 nm is in good agreement with the experimental results of 57 nm.

V. Conclusions

The absorption spectra of Prodan in water, acetonitrile, dichloromethane and cyclohexane are well described with different methods (INDO-CIS, TDDFT and CASPT2) and all agree that the first band is composed of three different electronic transitions, one dark -π* and two bright π-π*.

Multi-configurational calculations showed that the three excited states, S_1 (π-π*), S_2 (n-π*) and S_3 (π-π*) are very close to each other in energy at the Franck-Condon geometry and their equilibrium structures are planar in vacuum. No twist of the carbonyl or dimethylamine groups is observed and they are in the same plane as the naphthalene rings. It is shown that the two bright excited electronic states can be simultaneously populated in the absorption transitions of Prodan. The S_3 (π-π*) relaxes to stable equilibrium geometry, while the S_1 (π-π*) decays by internal conversion to the more stable S_2 (n-π*) state. These two states, S_2 (n-π*) and S_3 (π-π*), would then become fluorescent states. The π-π* S_3 state has a large dipole moment and is the higher energy (λ_1^{-1}) fluorescent state and the n-π* S_2 state has a small dipole moment and is the lower energy (λ_2^{-1}) fluorescent state. This information of larger dipole to the λ_1^{-1} transition is in agreement with the experimental data[10] that shows a larger contribution of λ_1^{-1} to the emission band in water comparatively to cyclohexane.

Additionally, the calculated energy shifts from vacuum to water are in the same direction as the experimental data, since the two emission transitions showed red shifts increasing solvent polarity.[10,14,15]

Hence, our combined experimental and theoretical studies point to a new explanation of the dual fluorescence of molecular probes. We conclude that the Prodan probe does not emit from a solvent-non-relaxed locally excited state and a relaxed twist or planar internal charge transfer excited state. Instead, it fluoresces from two different and independent excited states, S_2 and S_3, which can be populated when Prodan is excited at 344-362 nm. Finally, it should be mentioned that this work focuses on the Prodan molecule but, we contend that the dual fluorescence of the related Laurdan molecule could be understood with the same reasoning.

Availability of Data

The data that supports the findings of this study are available within the article and its supplementary information material.

Dedication

This paper honors Prof. Yvone Primerano Mascarenhas, a pioneer in the field of biomolecular structures in Brazil. With an outstanding capacity for teaching and mentoring, she inspired many students to pursue careers in biophysical chemistry thus helping to create important groups.

Acknowledgments

This work has been partially supported by the following Brazilian agencies and projects: FAPESP (2017/11631-2); CAPES for the BioMol project 23038.004630/2014-35; the National Institute of Science and Technology of Complex Fluids (INCT-FCx) with the CNPq grant 141260/2017-3 and FAPESP grant 2014/50983-3. CCV-S acknowledges fellowship supports from FAPESP 06/55513-9 and 10/08365-0. YOG acknowledges fellowship supports from FAPESP 12/15161-7. SC, MTL and KC acknowledge financial supports from CNPq.

References

1 G. Weber and F. J. Farris, Synthesis and Spectral Properties of a Hydrophobic Fluorescent-

Probe - 6-Propionyl-2-(Dimethylamino)Naphthalene, *Biochemistry*, 1979, **18**, 3075–3078.
2 T. Parasassi, F. Conti and E. Gratton, Time-Resolved Fluorescence Emission-Spectra of Laurdan in Phospholipid-Vesicles by Multifrequency Phase and Modulation Fluorometry, *Cell Mol Biol*, 1986, **32**, 103–108.
3 T. Parasassi, G. Destasio, G. Ravagnan, R. Rusch and E. Gratton, Quantitation of Lipid Phases in Phospholipid-Vesicles by the Generalized Polarization of Laurdan Fluorescence, *Biophys. J.*, 1991, **60**, 179–189.
4 F. Moyano, J. J. Silber and N. M. Correa, On the investigation of the bilayer functionalities of 1,2-di-oleoyl-sn-glycero-3-phosphatidylcholine (DOPC) large unilamellar vesicles using cationic hemicyanines as optical probes: A wavelength-selective fluorescence approach, *J Colloid Interf Sci*, 2008, **317**, 332–345.
5 L. A. Bagatolli, B. Maggio, F. Aguilar, C. P. Sotomayor and G. D. Fidelio, Laurdan properties in glycosphingolipid-phospholipid mixtures: A comparative fluorescence and calorimetric study, *Biochim. Biophys. Acta-Biomembranes*, 1997, **1325**, 80–90.
6 D. Marsh, Reaction Fields in the Environment of Fluorescent Probes: Polarity Profiles in Membranes, *Biophys. J.*, 2009, **96**, 2549–2558.
7 C. C. De Vequi-Suplicy, C. R. Benatti and M. T. Lamy, Laurdan in fluid bilayers: Position and structural sensitivity, *J Fluoresc*, 2006, **16**, 431–439.
8 J. Catalan, P. Perez, J. Laynez and F. G. Blanco, Analysis of the Solvent Effect on the Photophysics Properties of 6-Propionyl-2-(dimethylamino)naphthalene (PRODAN), *J Fluoresc*, 1991, **1**, 215–223.
9 J. R. Lakowicz, *Principles of Fluorescence Spectroscopy*, Plenum Publishers, New York, Third Edit., 2006.
10 C. C. Vequi-Suplicy, K. Coutinho and M. T. Lamy, New Insights on the Fluorescent Emission Spectra of Prodan and Laurdan, *J. Fluoresc.*, 2015, **25**, 621–629.
11 A. D. Lúcio, C. C. Vequi-Suplicy, R. M. Fernandez, M. T. Lamy, A. D. Lucio, C. C. Vequi-Suplicy, R. M. Fernandez, M. T. Lamy, Laurdan Spectrum Decomposition as a Tool for the Analysis of Surface Bilayer Structure and Polarity: a Study with DMPG, Peptides and Cholesterol, *J. Fluoresc.*, 2010, **20**, 473–482.
12 J. R. Lakowicz and A. Balter, Differential-Wavelength Deconvolution of Time-Resolved Fluorescence Intensities - a New Method for the Analysis of Excited-State Processes, *Biophys. Chem.*, 1982, **16**, 223–240.
13 J. R. Lakowicz and A. Balter, Analysis of Excited-State Processes by Phase-Modulation Fluorescence Spectroscopy, *Biophys. Chem.*, 1982, **16**, 117–132.
14 B. A. Rowe, C. A. Roach, J. Lin, V. Asiago, O. Dmitrenko, S. L. Neal, O. Dmitrenko, S. L. Neal, O. Dmitrenko and S. L. Neal, Spectral Heterogeneity of PRODAN Fluorescence in Isotropic Solvents Revealed by Multivariate Photokinetic Analysis, *J. Phys. Chem. A*, 2008, **112**, 13402–13412.
15 M. Raguz and J. Brnjas-Kraljevic, Resolved Fluorescence Emission Spectra of PRODAN in Ethanol/Buffer Solvents, *J. Chem. Inf. Model.* 2005, **45**, 1636–1640.
16 T. Parasassi, E. K. Krasnowska, L. Bagatolli and E. Gratton, LAURDAN and PRODAN as polarity-sensitive fluorescent membrane probes, *J. Fluoresc.*, 1998, **8**, 365–373.
17 A. Balter, W. Nowak, W. Pawelkiewicz, A. Kowalczyk, W. Pawełkiewicz and A. Kowalczyk, Some remarks on the interpretation of the spectral properties of prodan, *Chem. Phys. Lett.*, 1988, **143**, 565–570.
18 C. E. Bunker, T. L. Bowen and Y. P. Sun, A Photophysical Study of Solvatochromic Probe 6-Propionyl-2-(N,N-Dimethylamino)Naphthalene (Prodan) in Solution, *Photochem Photobiol*, 1993, **58**, 499–505.
19 B. Mennucci, M. Caricato, F. Ingrosso, C. Cappelli, R. Cammi, J. Tomasi, G. Scalmani and M. J. Frisch, How the environment controls absorption and fluorescence spectra of PRODAN: A quantum-mechanical study in homogeneous and heterogeneous media, *J Phys Chem B*, 2008, **112**, 414–423.
20 L. Cwiklik, A. J. A. Aquino, M. Vazdar, P. Jurkiewicz, J. Pittner, M. Hof and H. Lischka, Absorption and Fluorescence of PRODAN in Phospholipid Bilayers: A Combined Quantum Mechanics and Classical Molecular Dynamics Study, *J. Phys. Chem. A*, 2011, **115**, 11428–

11437.
21 A. M. Rollinson and H. G. Drickamer, High-Pressure Study of Luminescence from Intramolecular Ct Compounds, *J. Chem. Phys.*, 1980, **73**, 5981–5996.
22 W. Nowak, P. Adamczak, A. Balter and A. Sygula, On the Possibility of Fluorescence from Twisted Intramolecular Charge-Transfer States of 2-Dimethylamino-6-Acylnaphthalenes - a Quantum-Chemical Study, *Theochem-Journal Mol. Struct.*, 1986, **139**, 13–23.
23 R. Adhikary, C. A. Barnes and J. W. Petrich, Solvation Dynamics of the Fluorescent Probe PRODAN in Heterogeneous Environments: Contributions from the Locally Excited and Charge-Transferred States, *J Phys Chem B*, 2009, **113**, 11999–12004.
24 Y. P. Morozova, O. M. Zharkova, T. Y. Balakina and V. Y. Artyukhov, Effect of proton-donor solvent and structural flexibility of prodan and laurdan molecules on their spectral-luminescent properties, *J. Appl. Spectrosc.*, 2009, **76**, 312–318.
25 R. K. Everett, A. A. Nguyen, C. J. Abelt, H. A. A. Nguyen, C. J. Abelt, A. A. Nguyen and C. J. Abelt, Does PRODAN Possess an O-TICT Excited State? Synthesis and Properties of Two Constrained Derivatives, *J. Phys. Chem. A*, 2010, **114**, 4946–4950.
26 B. N. Davis and C. J. Abelt, Synthesis and photophysical properties of models for twisted PRODAN and dimethylaminonaphthonitrile, *J. Phys. Chem. A*, 2005, **109**, 1295–1298.
27 V. I. Tomin, Nonradiative energy transfer in a concentrated solution of prodan, *Opt. Spectrosc.*, 2006, **101**, 563–567.
28 V. I. Tomin and K. Hubisz, Inhomogeneous spectral broadening and the decay kinetics of the luminescence spectra of prodan, *Opt. Spectrosc.*, 2006, **101**, 98–104.
29 M. Novaira, M. A. Biasutti, J. J. Silber and N. M. Correa, New insights on the photophysical behavior of PRODAN in anionic and cationic reverse micelles: From which state or states does it emit?, *J. Phys. Chem. B*, 2007, **111**, 748–759.
30 P. Ilich and F. G. Prendergast, Singlet adiabatic states of solvated PRODAN: A semiempirical molecular orbital study, *J. Phys. Chem.*, 1989, **93**, 4441–4447.
31 A. B. J. Parusel, F. W. Schneider and G. Kohler, An ab initio study on excited and ground state properties of the organic fluorescence probe PRODAN, *J Mol Struc-Theochem*, 1997, **398**, 341–346.
32 M. Viard, J. Gallay, M. Vincent, O. Meyer, B. Robert and M. M. Paternostre, Laurdan solvatochromism: Solvent dielectric relaxation and intramolecular excited-state reaction, *Biophys. J.*, 1997, **73**, 2221–2234.
33 A. Parusel, Semiempirical studies of solvent effects on the intramolecular charge transfer of the fluorescence probe PRODAN, *J. Chem. Soc. Trans.*, 1998, **94**, 2923–2927.
34 A. B. J. J. Parusel, R. Schamschule, G. Köhler, G. Ko, A. B. J. J. Parusel, R. Schamschule and G. Kohler, Nonlinear optics. A semiempirical study of organic chromophores, *J. Mol. Struct. THEOCHEM*, 2001, **544**, 253–261.
35 K. A. Kozyra, J. R. Heldt, J. Heldt, M. Engelke and H. A. Diehl, Concentration and temperature dependence of Laurdan fluorescence in glycerol, *Z Naturforsch. A*, 2003, **58**, 581–588.
36 B. C. Lobo and C. J. Abelt, Does PRODAN possess a planar or twisted charge-transfer excited state? Photophysical properties of two PRODAN derivatives, *J. Phys. Chem. A*, 2003, **107**, 10938–10943.
37 M. Novaira, F. Moyano, M. A. Biasutti, J. J. Silber and N. M. Correa, An example of how to use AOT reverse micelle interfaces to control a photoinduced intramolecular charge-transfer process, *Langmuir*, 2008, **24**, 4637–4646.
38 A. Samanta and R. W. Fessenden, Excited state dipole moment of PRODAN as determined from transient dielectric loss measurements, *J. Phys. Chem. A*, 2000, **104**, 8972–8975.
39 E. Runge and E. K. U. Gross, Density-Functional Theory for Time-Dependent Systems, *Phys. Rev. Lett.*, 1984, **52**, 997–1000.
40 S. Miertus, E. Scrocco and J. Tomasi, Electrostatic Interaction of a Solute with a Continuum - a Direct Utilization of Abinitio Molecular Potentials for the Prevision of Solvent Effects, *Chem. Phys.*, 1981, **55**, 117–129.
41 J. Ridley and M. Zerner, Intermediate Neglect of Differential Overlap Technique for Spectroscopy - Pyrrole and Azines, *Theor. Chim. Acta*, 1973, **32**, 111–134.

42 J. Tomasi, Thirty years of continuum solvation chemistry: a review, and prospects for the near future, *Theor Chem Acc*, 2004, **112**, 184–203.
43 J. Tomasi, B. Mennucci and R. Cammi, Quantum mechanical continuum solvation models, *Chem. Rev.*, 2005, **105**, 2999–3093.
44 K. Andersson, P. A. Malmqvist and B. O. Roos, 2nd-Order Perturbation-Theory with a Complete Active Space Self-Consistent Field Reference Function, *J. Chem. Phys.*, 1992, **96**, 1218–1226.
45 F. Aquilante, L. De Vico, N. Ferre, G. Ghigo, P. A. Malmqvist, P. Neograd y, T. B. Pedersen, M. Pitonak, M. Reiher, B. O. Roos, L. Serrano-Andres, M. Urban, V. Veryazov and R. Lindh, Software News and Update MOLCAS 7: The Next Generation, *J. Comput. Chem.*, 2010, **31**, 224–247.
46 C. Centre, Theoretica Chimica Acta Density matrix averaged atomic natural orbital (ANO) basis sets for correlated molecular wave functions, *Theor. Chim. Acta*, 1990, **77**, 291–306.
47 P.-O. O. Widmark, B. Joakim, Persson, B. O. Roos, B. J. Persson and B. O. Roos, Density matrix averaged atomic natural orbital (ANO) basis sets for correlated molecular wave functions, *Theor. Chim. Acta*, 1991, **79**, 419–432.
48 C. C. Vequi-Suplicy, K. Coutinho and M. T. Lamy, Electric dipole moments of the fluorescent probes Prodan and Laurdan: experimental and theoretical evaluations, *Biophys. Rev.*, 2014, **6**, 63–74.
49 M. C. Zerner, ZINDO/UF: A semi-empirical program package, 2000, University of Florida, Gainesville/USA.
50 M. J. Frisch, G. W. Trucks, H. B. Schlegel, G. E. Scuseria, M. A. Robb, J. R. Cheeseman, J. A. Montgomery, T. V. Jr., K. N. Kudin, J. C. Burant, J. M. Millam, J. A. Pople, et al., 2004, GAUSSIAN 03.
51 G. Karlstrom, R. Lindh, P. A. Malmqvist, B. O. Roos, U. Ryde, V. Veryazov, P. O. Widmark, M. Cossi, B. Schimmelpfennig, P. Neograd y and L. Seijo, MOLCAS: a program package for computational chemistry, *Comput. Mater. Sci.*, 2003, **28**, 222–239.
52 K. Coutinho, S. Canuto and M. C. Zerner, A Monte Carlo-quantum mechanics study of the solvatochromic shifts of the lowest transition of benzene, *J. Chem. Phys.*, 2000, **112**, 9874–9880.
53 W. R. Rocha, K. Coutinho W. B. De Almeida and S. Canuto**,** An Efficient Quantum Mechanical/Molecular Mechanics Monte Carlo Simulation of Liquid Water, *Chem. Phys. Lett.* 2001, **335**, 127.
54 W. R. Rocha, V. M. Martins, K. Coutinho and S. Canuto, Solvent effects on the electronic absorption spectrum of formamide studied by a sequential Monte Carlo/quantum mechanical approach, *Theor. Chem. Acc.*, 2002, **108**, 31–37.
55 M. P. Allen and D. J. Tildesley, *Computer Simulation of Liquids*, Oxford University Press, Oxford, 1989.
56 W. L. Jorgensen, D. S. Maxwell and J. TiradoRives, Development and testing of the OPLS all-atom force field on conformational energetics and properties of organic liquids, *J. Am. Chem. Soc.*, 1996, **118**, 11225–11236.
57 H. C. Georg, K. Coutinho and S. Canuto, Converged electronic polarization of acetone in liquid water and the role in the n-pi* transition, *Chem. Phys. Lett.*, 2006, **429**, 119–123.
58 R. C. Barreto, K. Coutinho, H. C. Georg and S. Canuto, Combined Monte Carlo and quantum mechanics study of the solvatochromism of phenol in water. The origin of the blue shift of the lowest pi-pi* transition., *Phys. Chem. Chem. Phys.*, 2009, **11**, 1388–1396.
59 V. Manzoni, M. L. Lyra, R. M. Gester, K. Coutinho and S. Canuto, Study of the optical and magnetic properties of pyrimidine in water combining PCM and QM/MM methodologies, *Phys. Chem. Chem. Phys*, 2010, **12**, 14023.
60 K. Coutinho, H. C. Georg, T. L. Fonseca, V. Ludwig and S. Canuto, An efficient statistically converged average configuration for solvent effects, *Chem. Phys. Lett.*, 2007, **437**, 148–152.
61 C. M. Breneman and K. B. Wiberg, Determining Atom-Centered Monopoles from Molecular Electrostatic Potentials - the Need for High Sampling Density in Formamide Conformational-Analysis, *J Comp Chem*, 1990, **11**, 361–373.
62 N. Ferre and J. G. Angyan, Approximate electrostatic interaction operator for QM/MM

calculations, *Chem. Phys. Lett.*, 2002, **356**, 331–339.
63 Y. Orozco-Gonzalez, C. Bistafa and S. Canuto, Solvent Effect on the Stokes Shift and on the Nonfluorescent Decay of the Daidzein Molecular System, *J. Phys. Chem. A*, 2013, **117**, 4404–4411.
64 H. J. C. C. Berendsen, J. R. Grigera and T. P. Straatsma, The Missing Term in Effective Pair Potentials, *J. Phys. Chem.*, 1987, **91**, 6269–6271.
65 H. J. Bohm, I. R. Mcdonald and P. A. Madden, An Effective Pair Potential for Liquid Acetonitrile, *Mol. Phys.*, 1983, **49**, 347–360.
66 W. C. Swope, H. C. Andersen, P. H. Berens and K. R. Wilson, A computer simulation method for the calculation of equilibrium constants for the formation of physical clusters of molecules: Application to small water clusters, *J. Chem. Phys.*, 1982, **76**, 637–649.
67 H. J. C. Berendsen, J. P. M. Postma, W. F. Vangunsteren, A. Dinola and J. R. Haak, Molecular-Dynamics with Coupling to an External Bath, *J. Chem. Phys.*, 1984, **81**, 3684–3690.
68 K. Coutinho and S. Canuto, 2009, DICE: A Monte Carlo program for molecular simulation, University of São Paulo, SP, Brazil.
69 H. M. Cezar, S. Canuto and K. Coutinho, DICE: A Monte Carlo code for molecular simulation including Configurational Bias Monte Carlo method, *J. Chem. Inf. Model.* 2020, **60**, 3472−3488.
70 J. W. Ponder and F. M. Richards, An Efficient Newton-Like Method for Molecular Mechanics Energy Minimization of Large Molecules, *J Comp Chem*, 1987, **8**, 1016–1024.
71 C. E. Kundrot, J. W. Ponder and F. M. Richards, Algorithms for Calculating Excluded Volume and Its Derivatives as a Function of Molecular-Conformation and Their Use in Energy Minimization, *J Comp Chem*, 1991, **12**, 402–409.
72 H. C. Georg, K. Coutinho, and S. Canuto, Solvent effects on the UV-visible absorption spectrum of benzophenone in water: A combined Monte Carlo quantum mechanics study including solute polarization, *J. Chem. Phys.*2007, **1261,** 034507.
73 S. Canuto, K. Coutinho and D. Trzesniak, New developments in Monte Carlo/quantum mechanics methodology. The solvatochromism of beta-carotene in different solvents, *Adv Quantum Chem*, 2002, **41**, 161–183.
74 Y. Huang, X. Y. Li, K. X. Fu and Q. Zhu, New formulation for non-equilibrium solvation: Spectral shifts and cavity radii of 6-propanoyl-2(N,N-dimethylamino) naphthalene and 4-(N,N-dimethylamino) benzonitrile, *J. Theor. Comput. Chem.*, 2006, **5**, 355–374.